

UCLA

UCLA Electronic Theses and Dissertations

Title

Silicon Anode Materials for Lithium Ion Batteries By High Energy Ball Milling

Permalink

<https://escholarship.org/uc/item/0fn6m287>

Author

Chen, Weiguo

Publication Date

2018

Peer reviewed|Thesis/dissertation

UNIVERSITY OF CALIFORNIA

Los Angeles

Silicon Anode Materials for Lithium Ion Batteries

By High Energy Ball Milling

A thesis submitted in partial satisfaction
of the requirements for the degree Master of Science
in Chemical Engineering

by

Weiguo Chen

2018

ABSTRACT OF THE THESIS

Silicon Anode Materials for Lithium Ion Batteries

By High Energy Ball Milling

by

Weiguo Chen

Master of Science in Chemical Engineering

University of California, Los Angeles, 2018

Professor Yunfeng Lu, Chair

Silicon is one of the most promising anode material for lithium ion batteries in the future, since it has largest theoretical capacity. However, the capacity fading which results from volume expansion and unstable SEI prevent it from industrial application. In this thesis, we used high energy ball milling method to get Si nanoparticles efficiently with low cost to enhance their capacity. These Si nanoparticles were also composited with graphite to increase their capacity but not influence their cycling performance. In order to deal with their volume expansion, a carbon structure based on crosslinked polymer is designed. It proves that this carbon structure can largely improve their capacity and cycling performance. After 100 cycles, it can still have a capacity of 1051mAh/g.

The thesis of Weiguo Chen is approved.

Vasilios Manousiouthakis

Philippe Sautet

Yunfeng Lu, Committee Chair

University of California, Los Angeles

2018

Table of contents

1	Introduction and Background	1
1.1	Brief Introduction on Lithium Ion Batteries (LIBs)	1
1.2	Electrode Materials for LIBs	2
1.3	HEBM methods for nanoparticles	7
1.4	Crosslinked polymers and Chitosan.....	8
2	Method.....	10
2.1	Design and Synthesis	10
2.1.1	Si nanoparticles.....	10
2.1.2	Si nanoparticles-Graphite.....	11
2.1.3	Si nanoparticles-PI-Carbon (Si-PI-C).....	12
2.1.4	Si nanoparticles@crosslinked chitosan-carbon (Si-CC-C).....	14
2.2	Characterization	15
2.3	Electrochemical test	16
3	Results	16
3.1	Si and Si Nanoparticles by High Energy Ball Milling.....	16
3.2	Si 1000 rpm-graphite	23
3.3	Si 1000 rpm@PI-C	24
3.4	Si 1000 rpm@crosslinked chitosan-carbon	26

4	Future work.....	31
5	Conclusion.....	31
6	Reference.....	33

List of Figures

Figure 1. Comparison of LIBs with other batteries from Ref. 1	1
Figure 2. Charge and Discharge Mechanisms for LIBs from Ref.3	2
Figure 3. Scheme for the capacity fading of Si anode resulted from volume expansion from Ref.11	5
Figure 4. Scheme for High Energy Ball Milling Method from Ref.28.....	7
Figure 5. Structures of Crosslinked Polymers from Ref.30.....	8
Figure 6. Structure of Chitosan.....	9
Figure 7. Crosslinking Reaction of Chitosan and Glutaraldehyde from Ref.31	10
Figure 8. Scheme for the Synthesis of Polyimide.....	13
Figure 9. Scheme for Synthesis of Si@crosslinked chitosan.....	14
Figure 10. XRD patterns for Si materials	17
Figure 11. SEM Images for Si nanoparticles a) Si 1000 rpm b) Si 750 rpm c) pristine Si.....	18
Figure 12. Half Cell Performance for Or Si powders and Si nanoparticles (750 rpm and 1000 rpm)	19
Figure 13. Comparison of the performance of Si 1000 rpm at different loadings.....	21
Figure 14 Comparison of the performance of Si nanoparticles (1000 rpm) with different lithiation voltage	22

Figure 15. Performance of Si nanoparticle-graphite composite containing different percentage of Si	23
Figure 16. SEM image for Si 1000 rpm@PI-C	25
Figure 17. Performance of Si 1000 rpm@PI-C compared with Si 1000 rpm.....	26
Figure 18. TEM image for Si nanoparticles@chitosan.....	27
Figure 19. Comparison of stability of Si nanoparticles in water(a), PAA solution(b) and chitosan solution(c).....	28
Figure 20. SEM image for Si 1000 rpm@crosslinked chitosan	29
Figure 21. XRD pattern for Si 1000 rpm@crosslinked chitosan-carbon.....	30
Figure 22. Performance of Si 1000 rpm@crosslinked chitosan-carbon compared with Si 1000 rpm.....	30
Table 1. Theoretical capacity of different anode/cathode materials from Ref.4	3
Table 2. common crosslinked polymers	8

Acknowledgements

I would like to thank Professor Yunfeng Lu for his guidance in this project as well as his help and support for my research.

I will also give my thanks to Doctor Gen Chen, Doctor Haiping Wu and Wenyue Shi for their help in the experiments. Doctor Runwei Mo, Jie Ren and other members from Lu Lab gave me many constructive suggestions which I strongly appreciate as well.

1 Introduction and Background

1.1 Brief Introduction on Lithium Ion Batteries (LIBs)

Human cannot live without energy. What's more, it plays an increasingly important role since recent several hundred years. We need a complete solution for energy issues including energy sources and methods for energy storage and conversion. When it comes to energy storage methods, we have several different storage mechanisms and media, for example, lithium ion batteries, lead-acid batteries, etc.

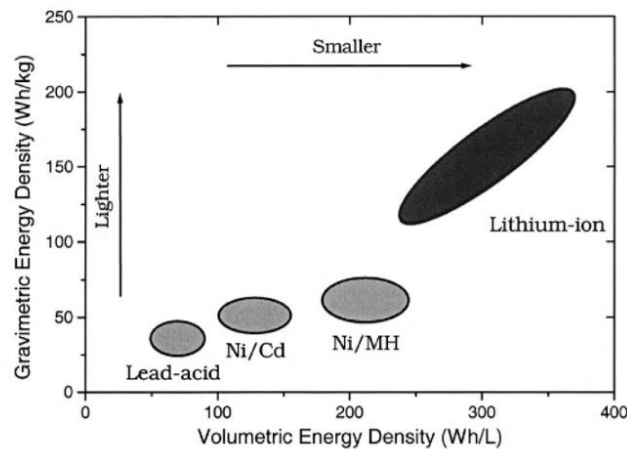


Figure 1. Comparison of LIBs with other batteries from Ref. 1

Among these Lithium ion batteries has become the most attractive energy storage devices nowadays. Compared with other batteries like lead-acid batteries or Ni/MH batteries, they have much larger gravimetric and volumetric capacity. They are portable and efficient in energy storage. Beside these, they have some other advantages, for instance, its ability to deliver high rates of power and its comparative low cost. Since then, they have been used to serve as power sources for digital devices like laptops or mobile phones.²

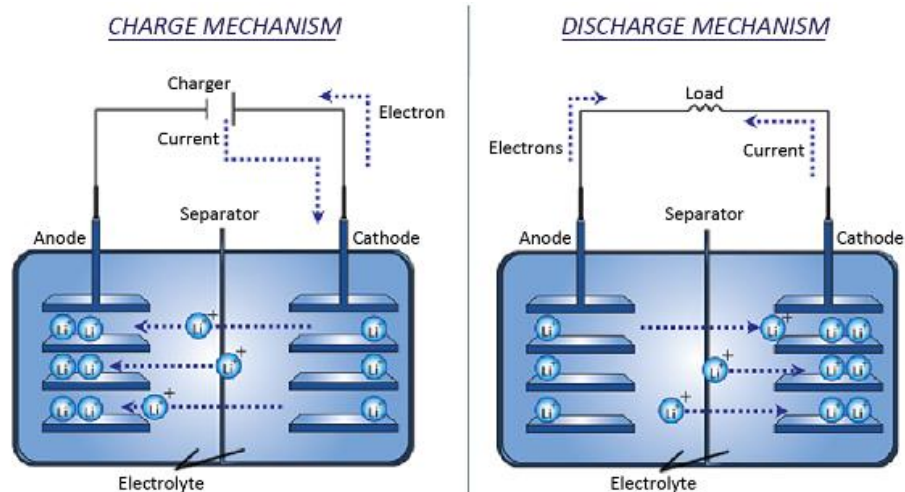


Figure 2. Charge and Discharge Mechanisms for LIBs from Ref.3

Here is a scheme that briefly shows the mechanism and configuration for commercial LIBs (Figure 2). These rechargeable lithium batteries involve a reversible insertion/extraction of lithium ions (guest species) into/from a host matrix (electrode material), called lithium insertion compound, during the discharge/charge process. The lithium insertion/extraction process occurring with a flow of ions through the electrolyte is accompanied by a reduction/oxidation(redox) reaction of the host matrix assisted with a flow of electrons through the external circuit. This process will happen between the anodes and the cathodes during cycles. Besides electrodes and electrolytes there are also separators. They are used to prevent the direct contact between anodes and cathodes, which will result in short circuit. However, they can permeate ions in electrolyte to make it conductive.

1.2 Electrode Materials for LIBs

Table 1. Theoretical capacity of different anode/cathode materials from Ref.4

materials	Anode/cathode	Theoretical capacity (mAh/g)	Level of Development
LiCoO ₂	Cathode	274	Commercialized
LiNi _{0.33} Mn _{0.33} Co _{0.33} O ₂	Cathode	280	Commercialized
Li ₂ MnO ₃	Cathode	458	Research
LiFePO ₄	Cathode	170	Commercialized
S	Cathode	1675	Research
Graphite	Anode	372	Commercialized
Li ₄ Ti ₅ O ₁₂	Anode	175	Commercialized
Si	Anode	4212	Research
Ge	Anode	1600	Research
Sn	Anode	990	Research

Here is the graph which briefly shows some electrode materials for LIBs (Table 1). For metal-based cathode materials, they have a theoretical capacity no more than 300 mAh/g. Sulfur have a theoretical capacity of 1675 mAh/g, which is much larger. And for anode materials, many of them are non-metal materials like Graphite, Silicon, and LTO is metal-based anode materials. However, commercialization need much more than theoretical capacity, when taking some other factors like recycling performance and cost into consideration, typically, we will use graphite as anode materials and metal oxides as cathode materials in industry currently. As I mentioned, these metal oxides materials have a typical theoretical capacity of 100~300 mAh/g. For graphite, it has a theoretical specific capacity of 372 mAh/g.⁵ Even though the capacity is comparatively low with

Sulfur or Silicon, their structures remain quite stable during charging and discharging, which ensure excellent cycling performance. It is sure that our current lithium ion batteries technology has many advantages, however, it cannot meet the energy requirement for some new applications like electric vehicles or hybrid vehicles. This has encouraged many scientists to put lots of efforts on developing electrodes with higher gravimetric and volumetric capacity for LIBs to surpass the energy density of the current ones. Significant research challenges and opportunities exist for all aspects of battery materials: cathode, anode, electrolyte, and separators. We will focus on the anode materials in this discussion.^{6,7}

If we take all materials into accounts, lithium metal has the largest theoretical capacity. However, safety issues like the occurrence of dendritic lithium during cycles prevent it from realistic applications, although scientists have put some efforts to deal with it.^{8,9} Therefore, from the graph above, we can conclude that Silicon is the best anode materials based on energy density consideration. For silicon, it can accommodate up to 4.4 lithium atoms per Silicon atoms, which gives it a capacity of 4212 mAh/g, 10 times larger than the current commercial anode material, graphite. Also, silicon is one of the most abundant element in the earth and it is non-toxic. What's more, it has a low discharge potential and a flat discharge platform, which is close to graphite and can provide stable power output during cycles. These similarities make silicon suitable for future commercialization. Moreover, silicon does not suffer from solvent co-intercalation, presenting an additional advantage over graphite.¹⁰

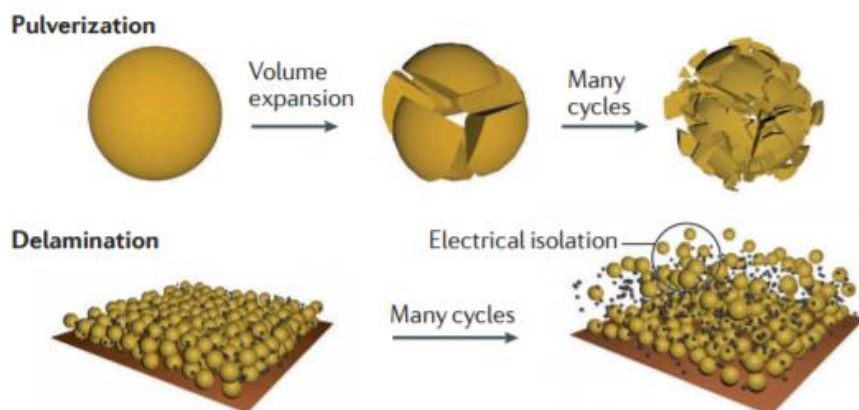


Figure 3. Scheme for the capacity fading of Si anode resulted from volume expansion from Ref.11

Even though silicon has so many comparatively advantages, it suffers from many disadvantages. First, they will experience a large volume expansion during lithiation. After fully lithiation, $\text{Li}_{4.4}\text{Si}$ has a volume about 3 times larger than origin Si. This volume change will be dangerous in closed batteries, which will lead to large internal stress inside the electrodes.¹²⁻¹⁵ This stress will compress Si particles and cause them to pulverize under such high pressure. After several cycles, origin Si particles will pulverize into much small particles. This graph shows the process of pulverization. One important result is the delamination of active materials. Original Si particles will have good contact with conductive materials like carbon and current collector. However, when turning into much smaller ones after many cycles, this close contact has also been destroyed. Many particles will fall off from electrode and cannot contribute to the capacity in the following cycles, which finally results in low cycling ability.¹⁶⁻¹⁸ Another main issue there is unstable Solid Electrolyte Interface (SEI) layer for Si anodes. Solid Electrolyte Interface is a layer structure between electrode materials and electrolytes since the first cycle. They are formed by reactions between lithium and electrolyte. However, the SEI for Si electrodes is fragile and unsteady. It will go broken then form new SEI. Because the formation of SEI layers will consume

lithium, this process will continually decrease the capacity and columbic efficiency at the same time.¹⁹⁻²² And also, smaller silicon particles produced by pulverization will also provide fresh lithium surface, further cause the loss of lithium. To conclude, unstable SEI and volume expansion these two factors combine together and result in low columbic efficiency and poor cycling performance for Si materials.

Notwithstanding, people has come up with several methods to overcome these problems. First, people try to move from bulk to nanoscale to reduce the stress. Scientists has make attempts on Silicon with different morphologies, including thin films, nanowires, nanotubes and nanoparticles. Obvious, Nanostructured materials also offer many benefits, including high rate capability due to the large surface area, short lithium diffusion distances within the electrode, and enhanced diffusion along surfaces and grain boundaries.²³

What's more important, these morphologies can minimize the total volumetric expansion, incorporating pores or voids to accommodate expansion, or by exploiting high surface-to-volume ratios to manage materials tress and therefore, improve the cycling performance. For example, we can wrap our Si nanoparticles with a layer of some other materials, which is several times larger than Si. Then the expansion will be confined in this shell and no longer cause large internal stress. People has developed different materials to wrap Si nanoparticles and largely improve the cycling performance.

Basically, there are two main materials to serve as shell. The first type is some hard materials, for instance, TiO₂.²⁴ These kinds of materials have better mechanic strength and stand the high stress. They can work with original SEI to build a stable composite SEI for Si materials and improve the cycling ability.

The second one is carbon materials. We can wrap Si nanoparticles with polymers then after annealing in high temperature, it would form a carbon shell on the surface of Si.²⁵⁻²⁷ These carbon shell is soft and elastic. What's more, it can help to improve the conductivity of component materials to enhance the performance, especially in high rate. And it is quite stable in most chemical and electrochemical conditions. Moreover, carbon coating is usually derived from common polymers, therefore their cost is reasonable for commercialization. These all make carbon the most widely used coating materials in chemistry.

1.3 HEBM methods for nanoparticles

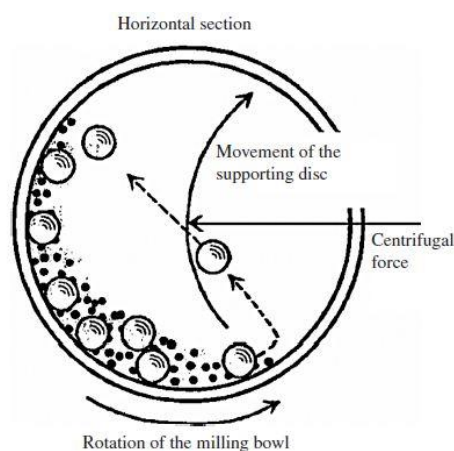


Figure 4. Scheme for High Energy Ball Milling Method from Ref.28

High Energy Ball Milling method is a common method to produce nanoparticles. It is a ball milling process where a powder mixture placed in the ball mill is subjected to high-energy collision from the balls. Their innovation has changed the traditional method in which production of materials is carried out by high temperature synthesis. Besides materials synthesis, it's also a way to get nanoparticles from bulk materials. furthermore, a way of inducing phase transformations in starting powders amorphization or polymorphic

transformations of compounds, disordering of ordered alloys, etc. During high-energy milling, the rapid collision applies large compressive force on the surface of your original materials, which afterwards cause the cracks on these raw particles. These cracks will grow up following and lead to fragmentation. Therefore, the size of materials will decrease to some critical values.²⁸

Further large energy supply to these crystals of limiting size causes further deformation of crystals, energy accumulation in the volume or at the surface of crystals, and subsequently amorphization.²⁹

1.4 Crosslinked polymers and Chitosan

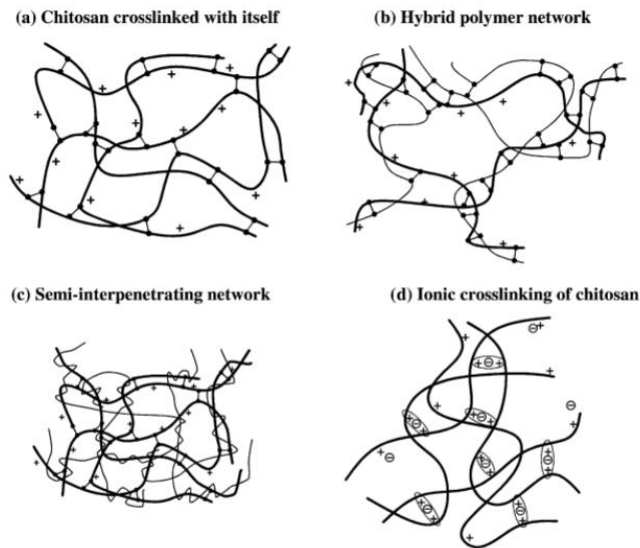
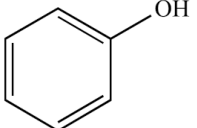
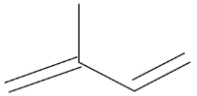
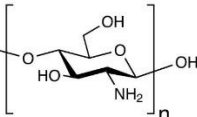
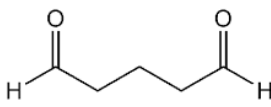


Figure 5. Structures of Crosslinked Polymers from Ref.30

Table 2. common crosslinked polymers

Name	Monomer	Crosslinking agent	Usage
------	---------	--------------------	-------

Phenol resin		HCHO
Rubber		Sulfur
Crosslinked chitosan		

A cross-link is a bond that links one polymer chain to another. They can be covalent bonds or ionic bonds. There are many kinds of crosslinking polymers, for example. Since here we use chitosan, we will focus on crosslinking methods for chitosan.

Chitosan is a copolymer of β -(1,4)-linked 2-acetamido-2-deoxy-D-glucopyranose and 2-amino-2-deoxy-Dglucopyranose. This polycationic biopolymer is generally obtained by alkaline deacetylation from chitin, which is the main component of the exoskeleton of crustaceans, such as shrimps. Chitosan is very common to produce crosslinked structures.

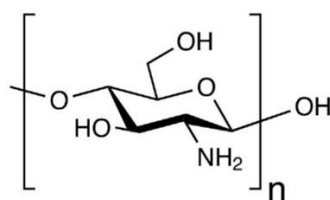


Figure 6. Structure of Chitosan

From their structure, we can see that chitosan have one amino group in every structure unit. Then this long chain polymer can be connected by chemicals with two or more function group.

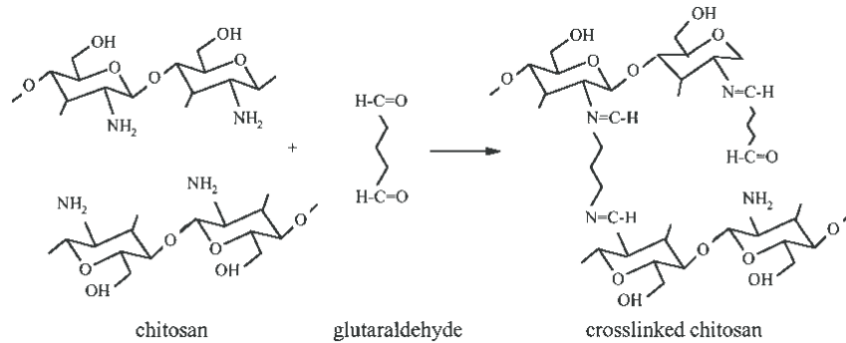


Figure 7. Crosslinking Reaction of Chitosan and Glutaraldehyde from Ref.31

The most widely used crosslinking agent for chitosan is Dialdehyde. They have two functional group, which can react with amino group to form covalent bonds.

2 Method

2.1 Design and Synthesis

2.1.1 Si nanoparticles

Even though Silicon nanoparticles can largely improve the capacity of bulk Si, their high price prevent it from commercialization and practical applications. Normally, Si nanoparticles are reduced by metal like Mg from SiO₂ nanoparticles. Since the size of original SiO₂ from hydrothermal method is quite uniform, the Si nanoparticles are nearly mono-distributed. However, Si nanoparticles synthesized by this method are expensive and they are unrealistic for industrial

usage. However, High Energy Ball Milling method is a very simple method to get nanoparticles efficiently and quickly. Si only experience physical collisions and we do not need any other process to purify our product. Also, the only cost is electrical energy. Since then, we choose it as our method to get Si nanoparticles.

Here is the synthesis of Si nanoparticles. Typically, 2g pristine Si powder was put into stainless vials(50ml), then 30g stainless ball (0.5mm). Then the vials were sealed under argon atmosphere to protect Si from being oxidized. Then the vials were put into the ball milling machine for operation. To protect ball milling machine, we set an operation procedure for it----- first 10 minutes Milling process then 10 minutes intersection. The total operation hour is 6 hours, which means the milling hour is 3 hours. Several different rotation speeds are applied to Si powders, for instance, 750 rpm and 1000 rpm. After Ball Milling, Si nanoparticles were directly used for following experiments. The yield for this method is more than 80%.

2.1.2 Si nanoparticles-Graphite

Even though Si-Majority Electrode can make the most use of its high capacity, industry has more consideration on the cost and cycle stability. Current Si anode cannot satisfy the industrial requirements because of their volume expansion and unstable SEI. However, these problems will not dominate when control the amount of amount of Si. As we mentioned, Si has a much larger capacity compare with graphite. What's more, the charge and discharge platform of Si and Graphite are similar, Si can be directly added into graphite without large changes in operation conditions. Therefore, here comes up with a simple idea to mix small amount of our Si nanoparticles with commercial graphite to enhance the overall capacity, but still maintain its cycling performance. In these conditions, the small amount of Si nanoparticles will evenly spread

inside graphite, where the stress resulted from volume expansion of Si will not play an important role. Eventually it leads to stable cycling performance. In these experiments, we want to find the most suitable proportion of Si nanoparticles in graphite.

Here is the experimental section. We take Si nanoparticles from ball milling method as our starting material. Here we also use ball milling machine to mix them with graphite, but with a lower rotation rate. Typically, a certain amount of Si nanoparticles (5%, 10% and 20%) will be added together with graphite then put into stainless vials. The total weight of graphite and Si is 2g. The ball we use here is the same as the former experiment. Then we seal the vial under argon atmosphere and operate ball milling machine at 400 rpm for 6h with the same operation procedure. Then composite materials were directly used as active materials for LIBs.

2.1.3 Si nanoparticles-PI-Carbon (Si-PI-C)

Polyimide(PI) is a common polymer. It can be obtained by the reaction between a dianhydride and a diamine (the most used method). Here are its structure and reactions.

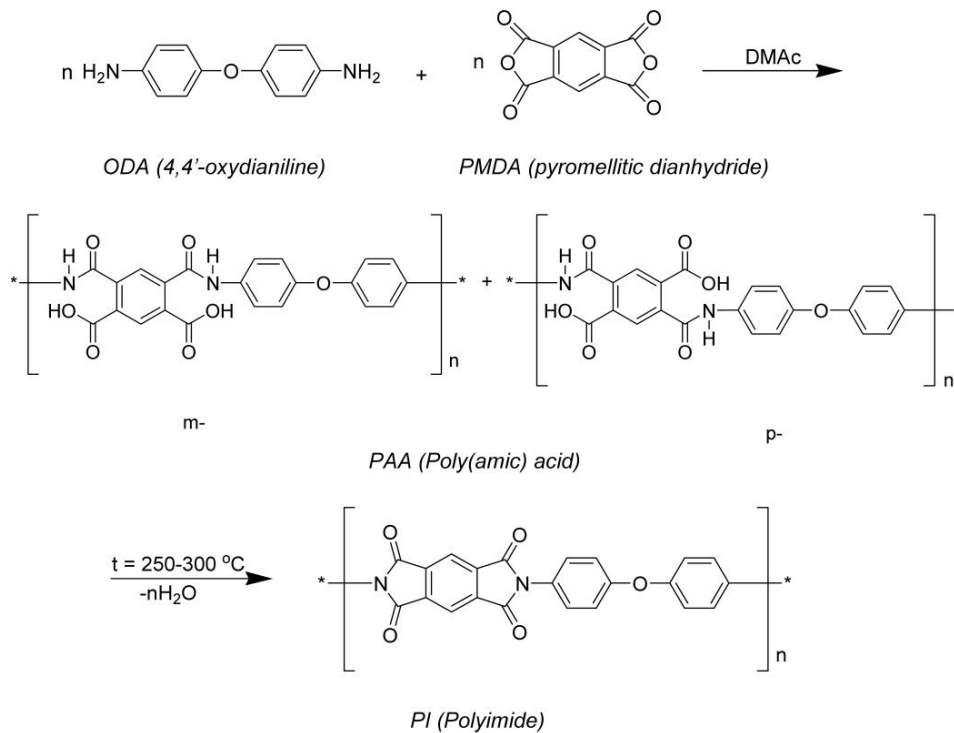


Figure 8. Scheme for the Synthesis of Polyimide

In industry and research, PI is known as engineering polymer for its thermal stability, good chemical resistance, excellent mechanical properties. Therefore, it is widely used in high temperature fuel cells, displays, and various military roles. Moreover, it can also be used as precursor for carbon nanostructures like carbon nanotubes. Unlike some other polymers like polyethylene and polypropylene, they can form dense carbon after annealing in high temperature. As we mention above, Si need carbon shell with void space to accommodate its volume expansion. The decomposition from polymer to carbon accompany with large weight loss, therefore it would wrap Si nanoparticles with dense layer of carbon with void space if we wrap Si nanoparticles with polyimide at first. However, polyimide is insoluble, so here we use its precursor, polyamide acid to wrap our Si nanoparticles. Also, the solution is quite vicious, which can stabilize the suspension.

First, Si nanoparticles are directly added into Polyamide acid DMF solution (10%), which is synthesized in previous. The weight ratio of Si BM and polyamide acid is 1:1. Then they are stirred for 30 min, then ultrasonicated for 30 min. Afterwards, dispersion is heated and stay at 150°C for 2 hours to remove the solvent. Then solid residue will be slowly heated and carbonized at 700 and 800 for 2 hours under Argon atmosphere.

2.1.4 Si nanoparticles@crosslinked chitosan-carbon (Si-CC-C)

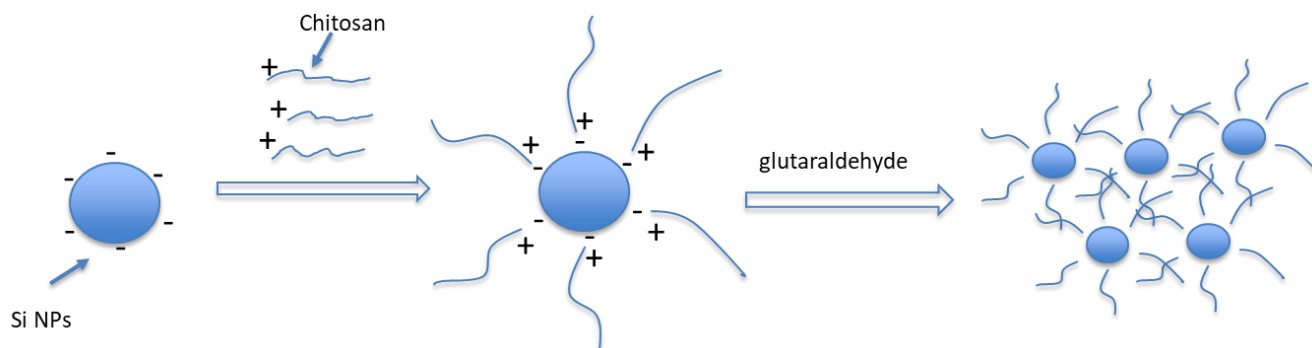


Figure 9. Scheme for Synthesis of Si@crosslinked chitosan

Si always has a thin layer of SiO_2 after exposing to the air because of their strong tendency to combine with oxygen. Therefore, the surface properties of Si are similar with SiO_2 . When disperse in the water, hydrogen atoms from water molecules will adhere to the surface. It makes oxygen atoms outside, which leads to negative charge on the surface. Since then, we come up with an idea to wrap individual Si nanoparticles with some polymers using the interaction between negative charge and positive charge. We can use a polymer with positive charge here, for example, chitosan. This can prevent Si nanoparticles from agglomeration to form a well-dispersed Si-polymer structure as the repulsive force between chitosan chains can stable this system in water.

Furthermore, we want to fix this well-dispersed structure to prevent the structure from being destroyed when removing the water. To achieve it, I try to introduce some crosslink agents to connect different chitosan chains and fix this structure. I use the most common and easy crosslinking method with the use of dialdehyde. The picture shows the synthesis scheme for it. After removing solvent under vacuum, finally we get a structure of Si nanoparticles@crosslinked chitosan.

Like many other polymer composites, Si nanoparticles@crosslinked chitosan can carbonize at high temperature under argon atmosphere to get Si@carbon structure. Since Si nanoparticles will disperse well in the polymer structure due to the repulsive force between chitosan chains, the Si nanoparticles can also disperse with the carbon structure. The carbon structure can improve the conductivity and make some void space to accommodate the volume expansion.

Here are the experimental steps. First, we solute chitosan in the HAc solution (1%) to get chitosan solution with a weight percentage of 5%. After completely dissolving chitosan, Si nanoparticles from ball milling are added into this solution. Again, we stir it for 30 mins and then ultrasonicate it for 30 mins to get a uniform dispersion. Glutaraldehyde solution is dilute from to 5%. Then Glutaraldehyde solution quickly adds into Si-chitosan dispersion, then immediately mix them up. Since the crosslink process will finish in 2 mins, we need to pay attention to it. Then we remove the water under vacuum to get a black film. This film can be further annealed to get Si-CC-C.

2.2 Characterization

The X-ray diffraction (XRD) measurements were taken by a Rigaku X-ray powder diffractometer with copper $K\alpha$ radiation ($\lambda = 1.54 \text{ \AA}$). During the analysis, the sample was scanned

from 5 to 80 ° at a speed of 5 degree per minute. Scanning electron microscopy (SEM) analysis was conducted on a JEOL JSM-6700F. Transmission electron microscopy (TEM) experiments were carried out on a Philips CM120 operated at 120 kV.

2.3 Electrochemical test

The Si, Si 750 rpm, and Si 1000 rpm electrode was prepared by mixing Si (70.0 wt%), 20.0 wt% conductive carbon black and 10.0 wt% poly(vinylidene fluoride) binder in N-methyl-2-pyrrolidinone solvent. For Si graphite composites, the ratio of active materials, carbon black and binder is 80% wt% : 10% wt% : 10% wt%. The obtained slurry was coated onto 15 mm thickness copper foil and dried at 60 °C in a vacuum oven for 12 h. The samples were then cut into 1 cm² disks at a mass loading of 0.6-1.2mg/cm². 2032 coin cells were assembled in an Ar-filled glovebox using these working electrodes with a polymer separator (Celgard 2250). Li metal was used as the counter electrode. 80 mL of 1.0 M LiPF₆ in 95 % 1 : 1 w/w ethylene carbonate/diethyl carbonate mixed with 5 % fluoroethylene carbonate was used as the electrolyte. For Si and Si@carbon batteries, they were activated at 0.2A/g (0.05C) for 5 cycles then were performed at 1A/g (0.25C). For Si-graphite composite, they were activated at 0.1A/g for 5 cycles then were performed at 0.2A/g. In the activation section, the lithiation voltage is from 1.50V to 0.01V. All the batteries tests were performed on LAND2000 battery tester.

3 Results

3.1 Si and Si Nanoparticles by High Energy Ball Milling

We use High Energy Ball Milling methods to get different samples. For the initial Si powder, the average size is 44 μ m. Here is the XRD pattern for our samples, the three strongest peak is on 28 °, 47 ° and 56 °.

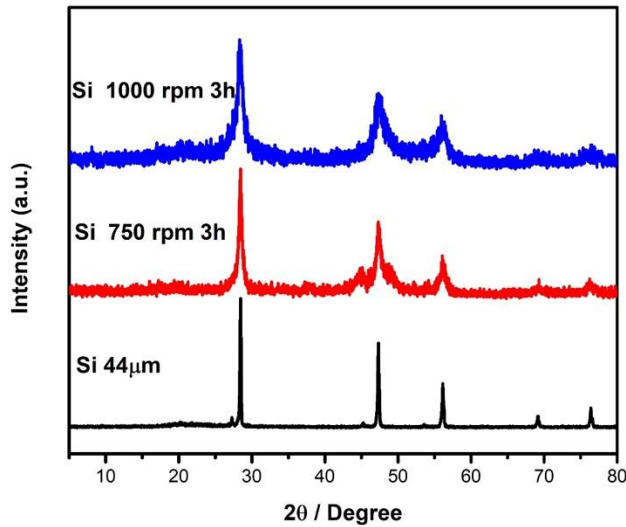


Figure 10. XRD patterns for Si materials

The pattern in the bottom represents for Si powders(44 μ m). We can see that the peak is sharp, which indicates its large crystal size. The two patterns above represent for samples operated by ball milling with different rotation rates. The red pattern is for 750 rpm and the blue one is for 1000 rpm. They are labeled as Si 750 rpm and Si 1000 rpm. Obviously, after ball milling for several hours, these peaks get much broader. The ball milling process first leads to the deformation of large particles which afterwards pulverize into much more smaller ones. Also, the milling process provide large energy for crystals and produce much more defects, which leads to the amorphization for Si particles. From Scherrer Equation, we can roughly estimate that the sizes of Si crystals are smaller than 20nm for both 750 rpm and 1000 rpm. Higher rotation rate result in further amorphization. However, XRD reflects the crystal size but not particles size. Also, under

such high pressure and high energy even though particles will pulverize at first, they can easily agglomerate afterwards. Therefore, the size of individual particles will much larger than crystal size. Actually, XRD data cannot directly tell us that the size of Si particles gets smaller, but it can be a supporting evidence.

To determine the particle size, we need SEM to give us direct information on particle size.

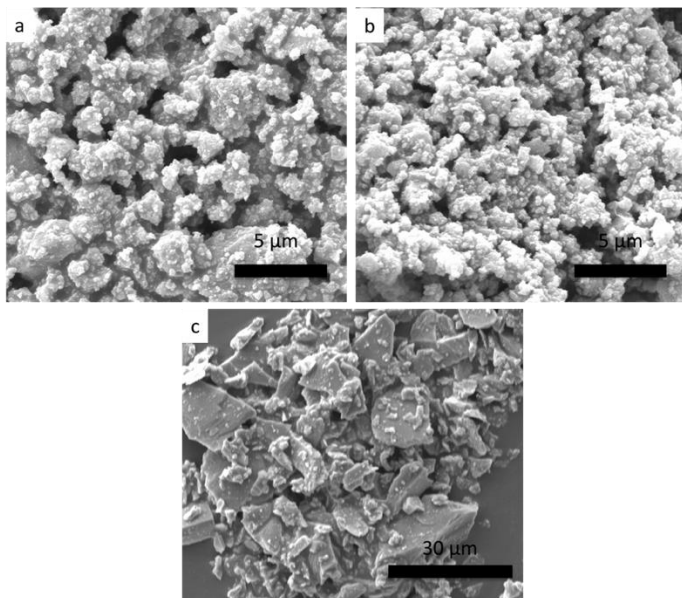


Figure 11. SEM Images for Si nanoparticles a) Si 1000 rpm b) Si 750 rpm c) pristine Si

Here is the SEM image for Si nanoparticles (750 rpm and 1000 rpm) and pristine Si powders. We can see the particle size is not so uniform since energy is not even applied to even Si particles. After ball milling, the size of most particles is less than 500 nm.

Then all these three samples-the origin Si powder, the sample after 750 rpm ball milling and the samples after 1000 rpm were use as active materials for LIBs anodes. Since our purpose is industrial application on EVs, all the battery test is under a high current density of $1\text{A}/\text{cm}^2$ (first 5 cycles $0.2\text{A}/\text{cm}^2$ for activation).

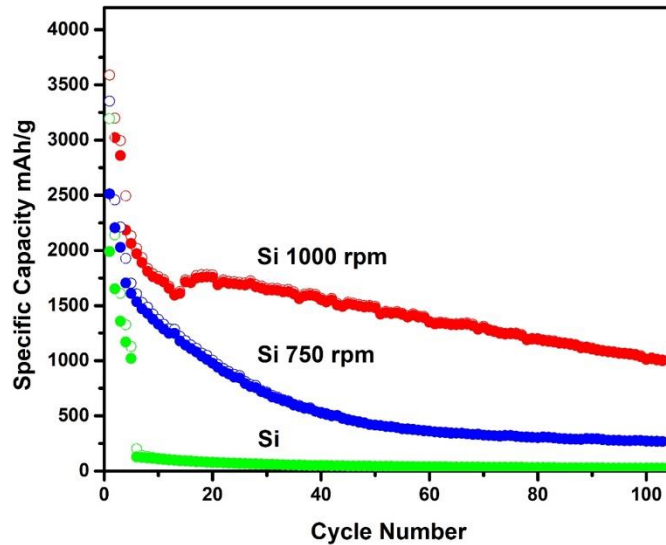


Figure 12. Half Cell Performance for Or Si powders and Si nanoparticles (750 rpm and 1000 rpm)

For the pristine Si powders, their capacity dramatically decreases after activation when. Since the pristine particles are large, surely the transportation of lithium ion might be a problem, especially at current density. But this is not the main reason. We also observe that the columbic efficiency is low for every cycle. These phenomena can be very well explained by the pulverization for Si particles. In first several cycles, the lithiation of anode result large volume expansion for Si particles, which causes extremely great stress inside the electrode. These particles cannot endure such large stress and then pulverize into small ones. During this process, many small particles do not will fall off from the electrode, then result in capacity fading. After few cycles, most active materials may lose their contact with current collector, which results in this dramatical capacity decrease. Moreover, for the remaining Si on the electrode, every pulverization will create fresh surface and then form new SEI layer. This is also a factor to lower the capacity and columbic efficiency since it continually consumes lithium. However, such dramatical capacity loss mostly result from the loss of electric contact.

Compare with pristine Si, the smaller size of ball milling samples makes it better for ion transfer. What's more, Si nanoparticles will have better contact with conductor like carbon. Even though that, at first several cycles the capacity of Si 750 rpm also fades rapidly due to the loss of active materials on the electrodes. However, the decrease will get much less after about 20 cycles. Next, along with the further consumption of lithium, their capacity will decrease in a slower rate.

For the Si 1000 rpm, the initial capacity is similar with the 750 rpm. However, the fading is rather slower than 750 rpm. As the size of particles is smaller, the active materials loss that resulted from the pulverization decrease. Also, when the size of Si particles gets smaller, the resistance for ion transfer get smaller, that's why we will get a maximum capacity after several cycles. After 20 cycles, the capacity is still fading, but with a stable rate. This can be accounted for the instability of SEI layer. Since the SEI is fragile, during every cycle part of SEI will break due to the expansion. Fresh electrode materials then expose to electrolytes. As we mentioned above, such process will consume "live" lithium, resulting in this decrease.

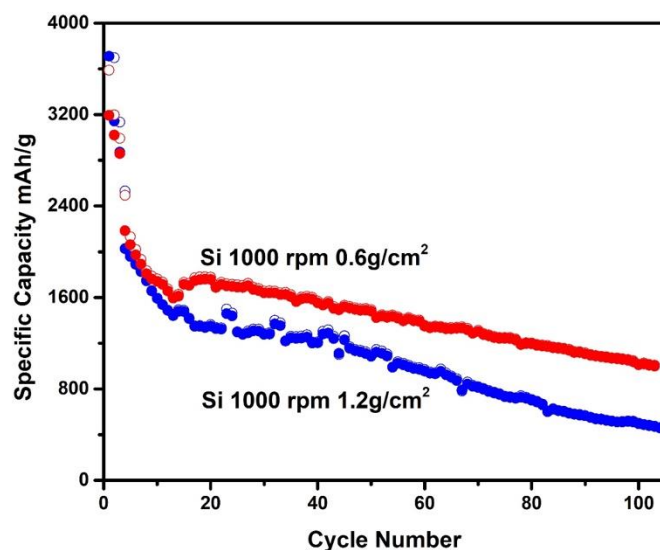


Figure 13. Comparison of the performance of Si 1000 rpm at different loadings

We also study the influence of different loading for electrodes (Figure 13.). Because the volume expansion is rather large, loading have really great impact on the electrochemical performance. We have electrodes with loadings of $0.6\text{g}/\text{cm}^2$ and $1.2\text{g}/\text{cm}^2$. For the electrode of $0.6\text{g}/\text{cm}^2$, expansion is comparatively smaller, and stress is smaller. Therefore, the loss of active materials from pulverization is less, and lead to higher retention. After 100 cycles, the capacity is 1040 mAh/g and 400 mAh/g respectively. The difference is obvious. That's why most Si majority have a loading less than $1\text{g}/\text{cm}^2$ and many are less than $0.5\text{g}/\text{cm}^2$. However, in such loading the areal capacity is too low to satisfy industrial requirements.

We all know that volume expansion comes from lithiation of Si. Since then, one method to control the large expansion is to control the extent of lithiation. As we mentioned, the complete lithiation will increase the volume by 3 times. However, if we stop the lithiation at some point after certain amount of expansion, we can also decrease the stress and reduce the pulverization. In

fact, it is easy to realize it by controlling the voltage to control the lithiation. In this experiment, I set the charge voltage from 1.5V to 0.1V instead of from 1.5V to 0.01V. The materials that we used here is Si nanoparticles (1000 rpm).

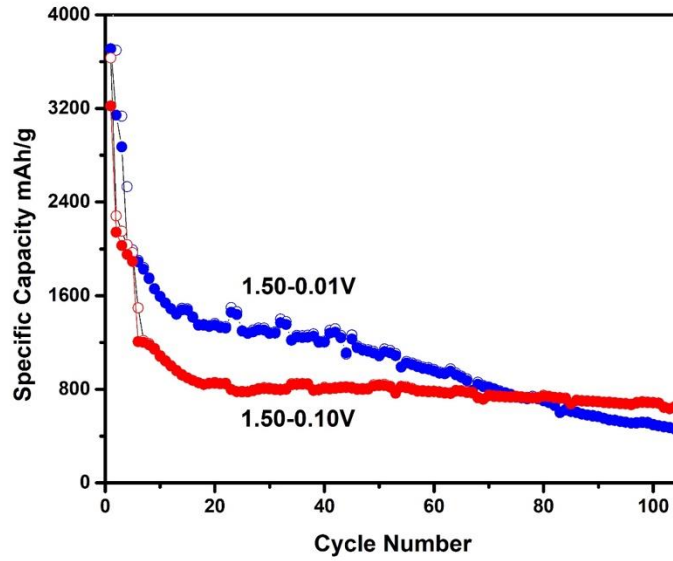


Figure 14 Comparison of the performance of Si nanoparticles (1000 rpm) with different lithiation voltage

The graph shows the comparison (Figure 14). After controlling the voltage, it can still have more than 70% of its former capacity. Then it will undergo a typical fading due to pulverization. However, after 20 cycles, the capacity become stable around 700 mAh/g at current density of 1A/g. The loading for it is 1.2g/cm², so the overall current density is 1.2 A/cm² and the overall areal capacity is 850 mAh/cm². For a typical coin cell with graphite anode, we have a current density of 0.4 A/cm² and 600 mAh/cm². By using this method, after 20 cycles, we can get an anode with larger capacity at a current density 3 times of graphite, which is promising for EVs.

In fact, the main consideration for Si is its cycling performance. It is meaningful to make it stable even though we may lose some capacity.

3.2 Si 1000 rpm-graphite

We can use this low-cost high energy ball milling method to get Si with comparative good performance, but it still need lots of efforts to meet industrial requirements. For example, we still need more than 10 cycles to stabilize our batteries. Also, the capacity loss in these cycles is more than 50%. Therefore, Si-majority anode is still on the stage of scientific research. However, we can combine it with our existing lithium batteries technology to quickly apply into industry. As we mentioned before, the charge voltage for Si is quite close to our commercial anode material, graphite. Therefore, we can make a composite of graphite and Silicon NP to combine their advantages together ---- increase the capacity but maintain its excellent cycling performance. Three different contents of Si NP are added into graphite then use ball milling to mix them up. For this part, we use a current density of 200 mAh/g, the same as commercial graphite anode.

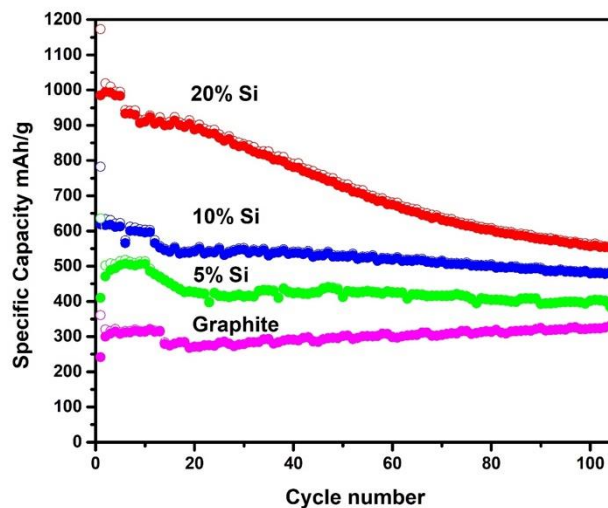


Figure 15. Performance of Si nanoparticle-graphite composite containing different percentage of Si

The graph shows the results of batteries test. The first one is sample with 5% Si. Compared with pure graphite, it can increase about one half of its original capacity. What's more, that's no big difference compared with pure graphite no matter on cycling retention or columbic efficiency. After further ball milling, all the Si NPs can be very well dispersed in the graphite. As Si nanoparticles is rather small and their volume percentage is small, the stress produced by volume expansion can be accommodate in the electrode. This result in no differences on cycling performance with pure graphite.

For the 10% sample, they have a capacity twice of original graphite. And we can see the retention is close to 90% after 100 cycles. What's more, the average columbic efficiency is more than 99.5%. These features show that even 10% Si is added into graphite, their stability remains. All these performances meet the requirement for full cell test and they can provide a much larger capacity than pure graphite.

Now turn to the sample with 20 % Si, it can increase the capacity for 600 mAh/g initially, about three times as graphite. Afterwards, we run this cell for over 100 cycles, we find that the battery will decrease and get a retention of % for 100 cycles. It could a good result but not enough for commercial full cell.

When compared the results of this series of experiments, we can conclude that for these unmodified Si nanoparticles which is simply produced by high energy ball milling, 10% Si should be the best choice.

3.3 Si 1000 rpm@PI-C

Since the direct use of Si nanoparticles as anode materials is still limited by their performance, we need some further modification to improve its performance and stability, especially at high loading. Also, our purpose is industrial application, the method should be rather simple and the cost should be controlled. We have tried direct wrapping of polymer then one-step high temperature annealing to finish carbon coating for Si nanoparticles.

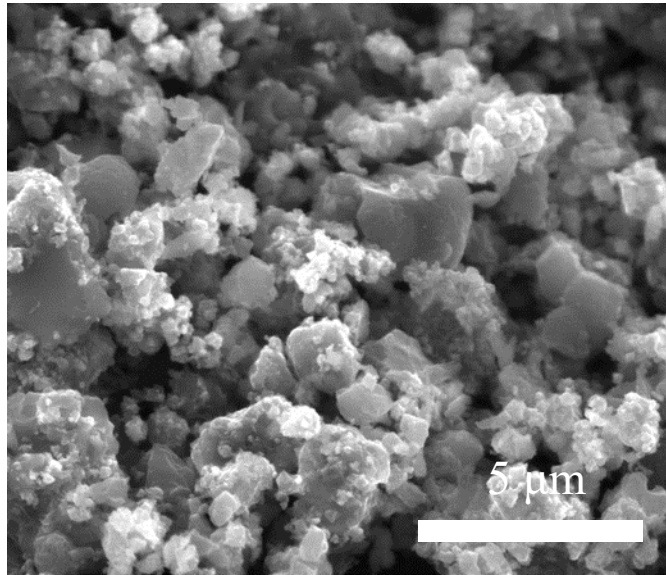


Figure 16. SEM image for Si 1000 rpm@PI-C

SEM images confirm that the size of these particles remain just unchanged (Figure 12). Here is their half cell performance compared with Si 1000 rpm.

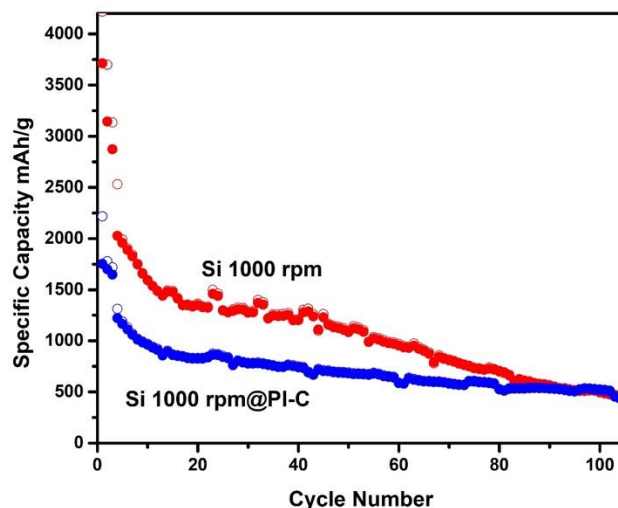


Figure 17. Performance of Si 1000 rpm@PI-C compared with Si 1000 rpm

We have compared their electrochemical performance with pure Si nanoparticles that we get from ball milling method. At the same loading, their initial capacity is 1700 mAh/g, which is lower than pure Si. However, their capacity decreases much slower. After 100 cycles, their capacity is even higher than pure Si. This shows that the carbon coating does improve the cycling performance for Si nanoparticles, even though this polymer or this strategy is not the best one. Therefore, we want to design a new structure to improve its performance.

3.4 Si 1000 rpm@crosslinked chitosan-carbon

In this experiment, the first step is to modify the surface of Si nanoparticles with Chitosan. After stirring and ultrasonicating, we take a little bit solution for TEM test to confirm our hypothesis.

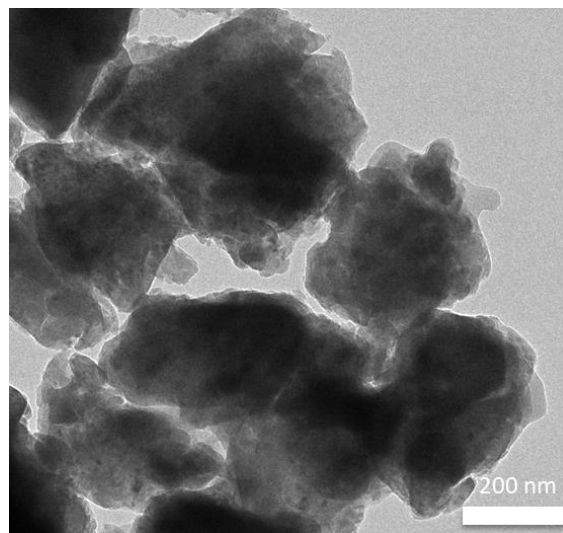


Figure 18. TEM image for Si nanoparticles@chitosan

From this image, we confirm that the size of our single Si particles is around 200 nm (Figure 18.). The dark part of these particles, which means high electron density, is Si. Also, all these Si particles are wrapped with a layer of lighter matter. This is polymer that has lower electron density.

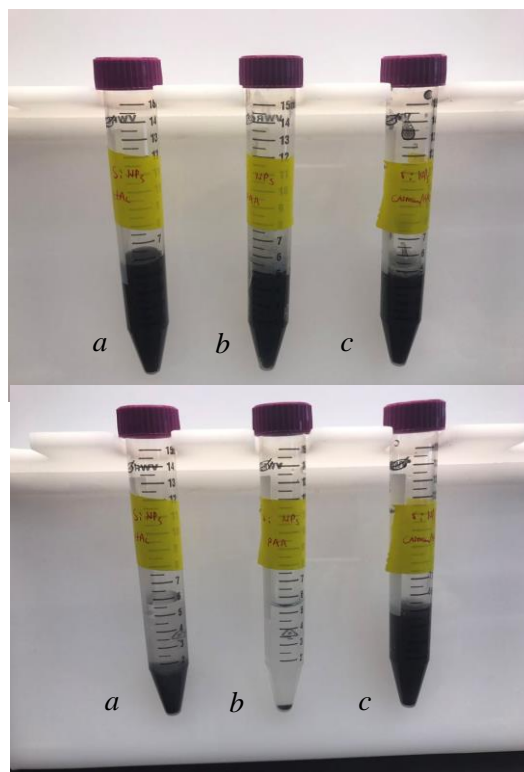


Figure 19. Comparison of stability of Si nanoparticles in water(a), PAA solution(b) and chitosan solution(c)

We have designed another experiment to show that such modification can help to prevent the aggregation of Si particles. Here we let our Si BM disperse in three different solutions, the first one is chitosan solution, the second one is water, and the last one is PAA solution (Figure 19.). All these dispersions were placed for 12h. From the picture, we compare their differences. The first one(a) is Si nanoparticles in water. Most of the Si nanoparticles participate after 12 hours, but the solution is not completely clear, which means that there is small amount of Si in the water. The second one(b) is PAA solution. PAA will dissociate in the water and then take negative charge, which have negative influence on stability. Therefore, the solution is completely clear. The last one(c) is our chitosan solution. After 12 hours, the solution remains unchanged when we compare the color. It shows that after wrapping with chitosan, the silicon particles can be really stable without aggregation in the water. To conclude, this experiment shows us that polymers with

different charges will play important roles here. Polymer with positive charge can wrap Si nanoparticles and protect them from aggregating, and polymer with negative charge will facilitate this process.

The next step is the crosslinking of chitosan to form this Si nanoparticles@crosslinked chitosan structure. We have tried with different concentration and found that it has significant impact on the crosslinking process. 5% glutaraldehyde will crosslink in five minutes after mixing up. Lower concentration takes hour to complete this process and higher concentration leads to an immediate crosslinking.

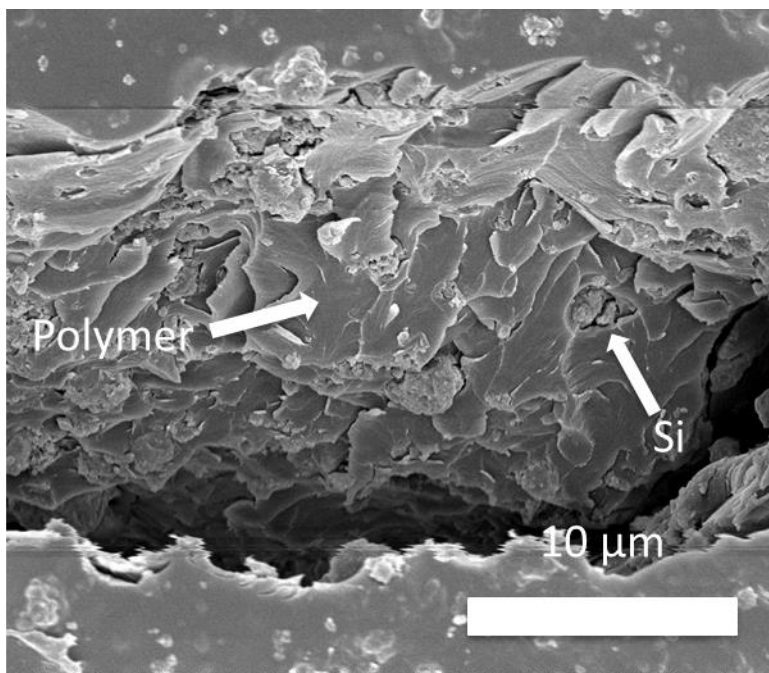


Figure 20. SEM image for Si 1000 rpm@crosslinked chitosan

We also have SEM image for Si@crosslinked polymers. We can see the small spherical particles, they are our Si NPs. These particles are distributed in these sheet-like structures. Then we anneal the Si composite sheet at 700 C under Argon atmosphere and take them as active material for battery test.

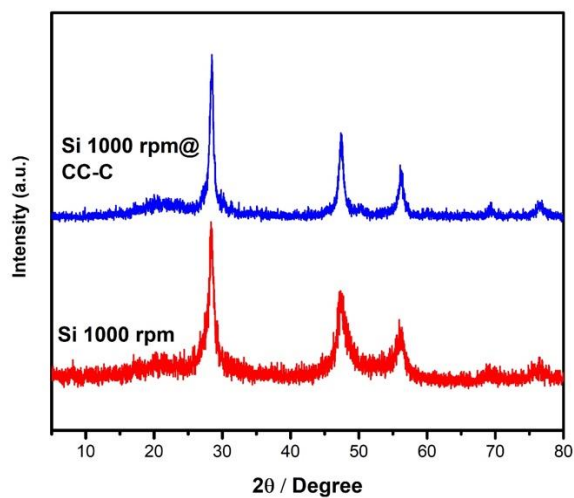


Figure 21. XRD pattern for Si 1000 rpm@crosslinked chitosan-carbon

Here shows their XRD patterns for annealed samples (Figure 21.).

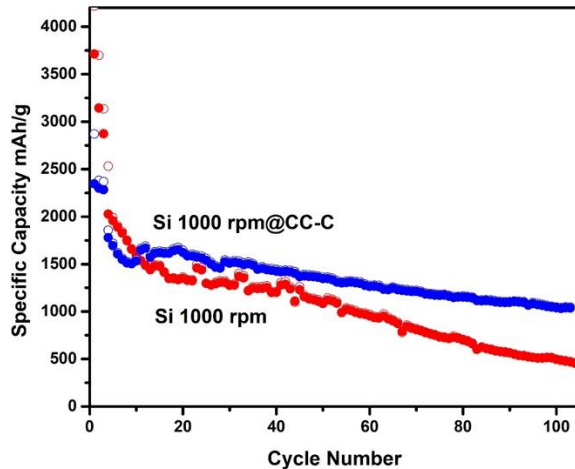


Figure 22. Performance of Si 1000 rpm@crosslinked chitosan-carbon compared with Si 1000 rpm

Here is the result of half cell test. TGA shows that weight percentage of Si in this composite is 70%. The initial capacity is around 2400 mAh/g and it is close to 70% of Si's theoretical capacity. Although in first several cycles its capacity is lower than pure Si nanoparticles, it decreases much

slower. After 110 cycles, this composite, Si 1000 rpm@crosslinked chitosan-carbon, has a capacity of 1040 mAh/g, which is 2.5 times of pure Si 1000 rpm. This result confirms our hypothesis that this carbon structure can markedly improve the cycling performance of Si anode materials as they can uniformly disperse Si nanoparticles and provide void space for volume expansion.

4 Future work

In the second part, we tested the performance of Si-Graphite composite materials. We have concluded that it would be a promising anode material for industrial use. I have done the half cell test and the next step is to use commercial NCM or LCO as cathode materials to perform their full cell test, then punch cell test.

In the last part of our experiment, we have designed Si nanoparticles@carbon structure to improve the cycling performance. The structure of this composite can accommodate the volume expansion and reduce local stress. Chitosan is used in this experiment. However, so other polymers and crosslinked polymer structures can also be used. Afterwards I can find out the best polymer structure for Si nanoparticles.

5 Conclusion

This thesis is aimed to design high-capacity anode materials with low cost. We selected Si as starting materials and used high energy ball milling to get Si nanoparticles. These nanoparticles provide much better cycling performance than pristine Si but still cannot meet industrial requirements. However, we can mix little amount of them with commercial anode material graphite to improve their capacity. The additive on of 10% Si to graphite will not influence its

cycling performance but double the capacity. Also, this thesis designed a carbon structure to accommodate the volume expansion of Si and improve the performance of Si majored anode, which is promising for EVs.

6 Reference

1. Nazri, G. A., & Pistoia, G. (Eds.). (2008). *Lithium batteries: science and technology*. Springer Science & Business Media.
2. Szczech, J. R., & Jin, S. (2011). Nanostructured silicon for high capacity lithium battery anodes. *Energy & Environmental Science*, 4(1), 56-72.
3. Mancini, M. (2009). *Improved anodic materials for lithium-ion batteries: surface modification by metal deposition and electrochemical characterization of oxidized graphite and titanium dioxide electrodes* (Doctoral dissertation, SCHOOL OF ADVANCED STUDIES-Doctorate course in Chemical sciences (XXI cycle)).
4. Nitta, N., Wu, F., Lee, J. T., & Yushin, G. (2015). Li-ion battery materials: present and future. *Materials today*, 18(5), 252-264.
5. Besenhard, J. O., Yang, J., & Winter, M. (1997). Will advanced lithium-alloy anodes have a chance in lithium-ion batteries?. *Journal of Power Sources*, 68(1), 87-90.
6. Owen, J. R. (1997). Rechargeable lithium batteries. *Chemical Society Reviews*, 26(4), 259-267.
7. Goodenough, J. B., & Kim, Y. (2009). Challenges for rechargeable Li batteries. *Chemistry of materials*, 22(3), 587-603.
8. Ding, F., Xu, W., Graff, G. L., Zhang, J., Sushko, M. L., Chen, X., ... & Liu, X. (2013). Dendrite-free lithium deposition via self-healing electrostatic shield mechanism. *Journal of the American Chemical Society*, 135(11), 4450-4456.
9. Khurana, R., Schaefer, J. L., Archer, L. A., & Coates, G. W. (2014). Suppression of lithium dendrite growth using cross-linked polyethylene/poly (ethylene oxide) electrolytes: a new

- approach for practical lithium-metal polymer batteries. *Journal of the American Chemical Society*, 136(20), 7395-7402.
10. Besenhard, J. O., Yang, J., & Winter, M. (1997). Will advanced lithium-alloy anodes have a chance in lithium-ion batteries?. *Journal of Power Sources*, 68(1), 87-90.
 11. Li, J. Y., Xu, Q., Li, G., Yin, Y. X., Wan, L. J., & Guo, Y. G. (2017). Research progress regarding Si-based anode materials towards practical application in high energy density Li-ion batteries. *Materials Chemistry Frontiers*, 1(9), 1691-1708.
 12. Limthongkul, P., Jang, Y. I., Dudney, N. J., & Chiang, Y. M. (2003). Electrochemically-driven solid-state amorphization in lithium-silicon alloys and implications for lithium storage. *Acta Materialia*, 51(4), 1103-1113.
 13. Li, J., & Dahn, J. R. (2007). An in situ X-ray diffraction study of the reaction of Li with crystalline Si. *Journal of The Electrochemical Society*, 154(3), A156-A161.
 14. Li, H., Huang, X., Chen, L., Zhou, G., Zhang, Z., Yu, D., ... & Pei, N. (2000). The crystal structural evolution of nano-Si anode caused by lithium insertion and extraction at room temperature. *Solid State Ionics*, 135(1-4), 181-191.
 15. B. Key, M. Morcrette, J. M. Tarascon and C. P. Grey, *J. Am. Chem. Soc.*, 2011, 133, 503–512.
 16. Wilson, A. M., & Dahn, J. R. (1995). Lithium insertion in carbons containing nanodispersed silicon. *Journal of The Electrochemical Society*, 142(2), 326-332.
 17. Yu, Y., Gu, L., Zhu, C., Tsukimoto, S., van Aken, P. A., & Maier, J. (2010). Reversible Storage of Lithium in Silver-Coated Three-Dimensional Macroporous Silicon. *Advanced Materials*, 22(20), 2247-2250.
 18. Liu, N., Wu, H., McDowell, M. T., Yao, Y., Wang, C., & Cui, Y. (2012). A yolk-shell design for stabilized and scalable Li-ion battery alloy anodes. *Nano letters*, 12(6), 3315-3321.

19. Erickson, E. M., Markevich, E., Salitra, G., Sharon, D., Hirshberg, D., de la Llave, E., ... & Aurbach, D. (2015). Development of advanced rechargeable batteries: a continuous challenge in the choice of suitable electrolyte solutions. *Journal of The Electrochemical Society*, *162*(14), A2424-A2438.
20. Etacheri, V., Geiger, U., Gofer, Y., Roberts, G. A., Stefan, I. C., Fasching, R., & Aurbach, D. (2012). Exceptional electrochemical performance of Si-nanowires in 1, 3-dioxolane solutions: a surface chemical investigation. *Langmuir*, *28*(14), 6175-6184.
21. Markevich, E., Fridman, K., Sharabi, R., Elazari, R., Salitra, G., Gottlieb, H. E., ... & Aurbach, D. (2013). Amorphous columnar silicon anodes for advanced high voltage lithium ion full cells: dominant factors governing cycling performance. *Journal of The Electrochemical Society*, *160*(10), A1824-A1833.
22. Markevich, E., Salitra, G., Rosenman, A., Talyosef, Y., Aurbach, D., & Garsuch, A. (2014). High performance of thick amorphous columnar monolithic film silicon anodes in ionic liquid electrolytes at elevated temperature. *RSC Advances*, *4*(89), 48572-48575.
23. Song, T., Xia, J., Lee, J. H., Lee, D. H., Kwon, M. S., Choi, J. M., ... & Zang, D. S. (2010). Arrays of sealed silicon nanotubes as anodes for lithium ion batteries. *Nano letters*, *10*(5), 1710-1716.
24. Jin, Y., Li, S., Kushima, A., Zheng, X., Sun, Y., Xie, J., ... & Shi, F. (2017). Self-healing SEI enables full-cell cycling of a silicon-majority anode with a coulombic efficiency exceeding 99.9%. *Energy & Environmental Science*, *10*(2), 580-592.
25. Liu, N., Wu, H., McDowell, M. T., Yao, Y., Wang, C., & Cui, Y. (2012). A yolk-shell design for stabilized and scalable Li-ion battery alloy anodes. *Nano letters*, *12*(6), 3315-3321.

26. Wu, H., Zheng, G., Liu, N., Carney, T. J., Yang, Y., & Cui, Y. (2012). Engineering empty space between Si nanoparticles for lithium-ion battery anodes. *Nano letters*, *12*(2), 904-909.
27. Li, X., Gu, M., Hu, S., Kennard, R., Yan, P., Chen, X., ... & Liu, J. (2014). Mesoporous silicon sponge as an anti-pulverization structure for high-performance lithium-ion battery anodes. *Nature communications*, *5*, 4105.
28. Suryanarayana, C. (2001). Mechanical alloying and milling. *Progress in materials science*, *46*(1-2), 1-184.
29. Baláž, P. (2008). High-energy milling. In *Mechanochemistry in Nanoscience and Minerals Engineering* (pp. 103-132). Springer Berlin Heidelberg.
30. Berger, J., Reist, M., Mayer, J. M., Felt, O., Peppas, N. A., & Gurny, R. (2004). Structure and interactions in covalently and ionically crosslinked chitosan hydrogels for biomedical applications. *European Journal of Pharmaceutics and Biopharmaceutics*, *57*(1), 19-34.
31. Öztop, H. N., Saraydin, D., & Cetinus, Ş. (2002). pH-sensitive chitosan films for baker's yeast immobilization. *Applied biochemistry and biotechnology*, *101*(3), 239-249.